The role of metalloporphyrins on the physical-chemical properties of petroleum fluids

Ana C R Sodero, Jean-Pierre Korb, Ahmad Alfarra, Pierre Giusti, Isabelle Baraille, Brice Bouyssière, Germain Vallverdu, Didier Bégué, Hugo Santos Silva

Fuel 188 (2017) 374–381

Contents lists available at ScienceDirect

Fuel

journal homepage: www.elsevier.com/locate/fuel

Full Length Article

The role of metalloporphyrins on the physical-chemical properties of petroleum fluids

Hugo Santos Silva [a,*], Ana C.R. Sodero [b], Jean-Pierre Korb [c], Ahmad Alfarra [d,e], Pierre Giusti [d,e], Germain Vallverdu [a,e], Didier Bégué [a,e], Isabelle Baraille [a,e], Brice Bouyssiere [a,e]

[a] Université de Pau et des Pays de l'Adour, IPREM (CNRS-UMR 5254), 2 Avenue Président Angot, 64053 Pau, France
[b] Laboratório de Modelagem Molecular e QSAR (MODMOLQSAR), Departamento de Fármacos e Medicamentos, Universidade Federal do Rio de Janeiro (UFRJ), Av. Carlos Chagas Filho, 373, 21941-599, Brazil
[c] Physique de la Matière Condensée, École Polytechnique-Centre National de la Recherche Scientifique (CNRS), 91128 Palaiseau, France
[d] Total Research & Technology, Gonfreville, BP 27, F-76700 Harfleur, France
[e] Joint Laboratory C2MC: Complex Matrices Molecular Characterization, Total Research & Technology, Gonfreville, BP 27, F-76700 Harfleur, France

ARTICLE INFO

Article history:
Received 20 September 2016
Received in revised form 6 October 2016
Accepted 11 October 2016
Available online 15 October 2016

Keywords:
Petroporphyrins
Aggregation
Asphaltenes
Molecular dynamics
Petroleum fluids

ABSTRACT

The presence of metalloporphyrins in crude oil has been known by many years now but their role on the physical-chemical properties of petroleum fluids, such as the aggregation of the high-molecular weight phases, remains unknown. In this paper, these properties are studied using different molecular modeling techniques (Molecular Dynamics, Semi-empirical PM7 and Density Functional Theory). This combined methodology allowed us characterizing the nature of these interactions, how it dominates the electronic structure of the stacked molecules and what is their participation on the formation of the nano-, micro- and macro-aggregates.

1. Introduction

Processing heavy crude oil has become of uppermost importance in oil industry. Refining these fractions allows one obtaining low-molecular weight distillates by catalytic and non-catalytic conversion [1–4]. The presence of metals in these fractions is known since the early '50s [5–9]. These metallic centers are found complexed in tetrapyrolic macrocycles (porphyrin derivatives) [10] and have a major negative impact during the phases of oil processing, since they can contaminate and deactivate the catalysts used in the refinery [11,12]. Moreover and very recently, it has been pointed out that these metalloporphyrins might play a major role on the asphaltene aggregation, being somehow trapped by these high-molecular weight oil's fractions [13]. This physico-chemical process is of remarkable interest in oil industry since, if not controlled, it can induce problems in several fields of petroleum utilization, from oil recovery and transportation to refining [14]. These complications arise from their tendency to aggregate out of solution, increasing oil viscosity, adsorption on solid surfaces, precipitation, etc. [15,16].

The asphaltene molecules consist of a complex mixture of polycyclic aromatic hydrocarbons substituted with alkyl side chains and the presence of heteroatoms, like nitrogen, sulfur and oxygen is common in the conjugated core [17–22]. Porphyrins also make part of this crude oil's polar fraction. Fourier transform ion cyclotron resonance mass spectroscopy (FT-ICR-MS) results indicate that they can bear either nickel, vanadium or iron as metallic centers [9,12,13,23–30]. Besides the fact that the asphaltene composition changes for different oil sources, the relative porphyrin contents are not constant across different oil sources [31–35]. Some crudes are richer in metals, namely nickel or vanadium, and up to our knowledge, no clear clue on their role on the aggregation has been proposed [16,36].

Size exclusion microchromatography with high-resolution inductively coupled plasma mass spectrometric detection technique (ICP-MS) has demonstrated the trapping of metalloporphyrins (MP) by asphaltene nanoaggregates [16]. Caumette et al. [37] and Barbier et al. [38] have shown using the same technique that nickel and vanadium can be found trapped in asphaltene aggregates with a mass range between 200 and 40,000 Da, in dif-

* Corresponding author.
E-mail address: hugo.santos-silva@univ-pau.fr (H. Santos Silva).

http://dx.doi.org/10.1016/j.fuel.2016.10.065
0016-2361/

ferent fractions with proportions that depends on the geographical or geochemical origin of the crude oil under study. More particularly, electron-spin resonance (ESR) quantitatively measured levels of the paramagnetic vanadyl ions VO^{2+} and organic radicals trapped in crude oils with and without asphaltene [16]. Moreover, pulsed ESR spectroscopy has identified a porphyrinic structure of the vanadium (IV) in the asphaltene for several crude oils through the coupling with the four neighboring nitrogens [39]. Both ESR and high-resolution mass spectroscopy have shown that around 2/3 of the VO^{2+} is trapped in MP embedded within asphaltene nanoaggregates while 1/3 stays in the bulk [16]. Recent experiments of nuclear magnetic relaxation dispersion (NMRD) in crude oils with asphaltenes have proven useful for characterizing the translational diffusion of maltenes at proximity of asphaltene nanoaggregates including trapped VO^{2+} paramagnetic sources of relaxation [16,40,41].

Basically, in NMRD techniques, the proton Larmor frequency ω_1 is varied allowing an exploration of the time scales of the magnetic fluctuations (noise) to which the longitudinal proton spin relaxation $1/T_1$ is sensitive [16,40]. Further, the magnetic field dependence of $1/T_1$ provides a good test of the theories that relate the measurement to the microdynamical behavior of the fluid. This is still true in complex fluids, such as crude oil, where the effect of reduced dimensionality may force more frequent reencounters of proton-spins bearing hydrocarbons with either paramagnetic species or proton-surface groups on asphaltene nanoaggregates. The remarkable observed features of the nuclear magnetic relaxation dispersion (NMRD) profiles of proton $1/T_1$ for bulk and confined crude oils with and without asphaltene have been interpreted with an original relaxation model of intermittent surface dynamics of proton species at the surface of asphaltene nanoaggregates and bulk dynamics in between the slowly rotating clusters of these nanoaggregates [40,41]. This allows probing the 2D translational diffusion correlation time as well as the time of residence of the hydrocarbons at the surface of the asphaltene nanoaggregates. The latter time gives an average radius of exploration, $r_{2D} \approx 3.5$ nm, for the 2D diffusion of hydrocarbons (maltenes) at proximity of the surface of asphaltene nanoaggregates that agrees with the sizes found previously by SAXS and SANS studies [42]. These NMRD experiments results are thus important for understanding the role of asphaltenes in the dynamics and hydrodynamics of crude oils confined in rocks. An immediate consequence of this experimentally observed 2D diffusion of hydrocarbons (maltenes) at proximity of the surface of asphaltene nanoaggregates is the existence of an attractive potential interaction between the maltene and asphaltene nanaoaggregates. One of our aims here is to find from our MD simulations the origin of such an attractive interaction for the vanadyl-containing porphyrins.

In silico, and up to our knowledge, no study has yet addressed the effect of these metallic centers on the asphaltene aggregating process and on other physical-chemical effects. Most of this is due to the need of using Classical Molecular Dynamics Simulations (CMDS) to study this phenomenon, but the parameters for metal centers are rare in number, quality and variety. Moreover, the structure of these porphyrinic and asphaltenic compounds is weakly resolved and a big effort has been done in our group in this sense [41,43,44]. Experimentally, a recent study has proposed the synthesis of nickel porphyrins having —COOH functions grafted to it in order to study the aggregation mechanism with asphaltenes but only intermediated by this polar function [45].

Iron and nickel molecular dynamics parameters are known and have already been published in several reports, being able of reproducing very well experimental data [46,47]. The former has been an intense object of study because of its presence in hemoglobin and several force fields present parameters for it [48]. Nickel parameters are rarer but can be found in late '90s reports, although they are only a few [49]. However, for the case of vanadium, as it is found as the vanadyl radical cation, no classical molecular dynamics parameter set can be found for it or can be either produced because of its radical character. Although this limitation, we pursue our wish to acquire more information on their role in the aggregation process and we propose a simple way to introduce classical molecular dynamics parameters for the vanadyl group. To circumvent this weakness of CMDS, we use Density Functional Theory (DFT) and the semi-empirical PM7 hamiltonian (PM7) calculations to validate the results obtained by the former. Moreover, for the case of vanadyl radical cation, the use of DFT and PM7 allowed us to explicitly take into account any possible effect due to the unpaired electron for which CMDS cannot account. This multi-scale approach herein presented proved then to be essential for studying the aggregation of asphaltene in the presence of metals.

2. Methodology

The computational details behind the classical molecular dynamics simulations (CMDS) are fully exposed in the ESI. We used two molecular models to study asphaltene's behavior, both of them of the "island"-type [50]. The first, called C5Pe (Fig. 1) is a N-(1-Hexylheptyl)-N′-(5-carboxy-licpentyl)-perylene-3,4,9,10-tetracarboxylicbis-imide derivative and was chosen since it has already proved to be a good model for asphaltenes besides the possibility of theory-experience confrontation due to its synthetic availability [51,52]. The second, called A13, is derived from the experimental work of molecular cartography done by Schueler et al. [53] which isolated and identified it using Atomic Force Microscopy (AFM). The behavior in solution and the aggregation of these molecules were studied and published recently by our group [43,44]. We took a simple porphyrin model bearing a metallic center to model the metalloporphyrins that can be found in crude oil. As the experimental molecular structure of these metallic compounds is weakly determined, we preferred not to introduce long alkyl lateral chains grafted on the conjugated core in order to study the effect on the

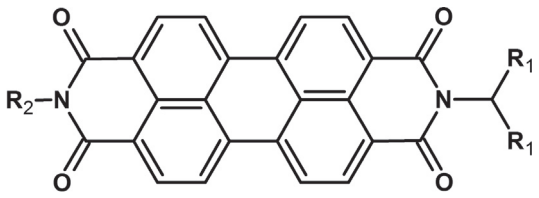

(a) C5Pe molecule

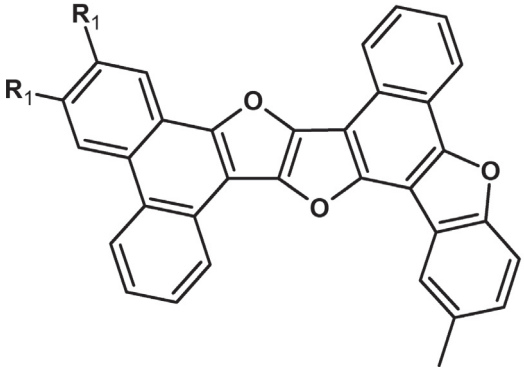

(b) A13 molecule

Fig. 1. Molecular structure of (a) C5Pe and (b) A13 molecules studied in this paper. R_1 is a n-C_6H_{13} chain and R_2 is a n-$(CH_2)_5COOH$ one.

aggregation of the metallic center only. These structures are depicted in Fig. 2.

DFT calculations were also performed to account for the missing formalism in CMDS. The details behind these calculations are fully explained in the ESI. Last but not least, **PM7 calculations** [54–57] were also performed as a middle-step between DFT and CMDS. More details are presented within the text and in the ESI.

3. Results and discussion

3.1. Classical Molecular Dynamics Simulations (CMDS)

CMDS started by determining the aggregation behavior of simulation boxes containing only one type of molecule at a time. This constitutes the baseline that allows one to say how the metalloporphyrins can have an effect on asphaltene aggregation or not. $5 \times 5 \times 5$ nm^3 simulation boxes containing either 2, 5 or 8 molecules of C5Pe, A13, or each one of the porphyrins were constructed and simulated. The aggregation within these systems were studied by the Radial Distribution Functions (RDFs), which allows one determining the probability of finding a molecule j, x nm away of a reference molecule i, during the whole simulation time.

Asphaltene-like molecules, such as C5Pe and A13, aggregate by both π-stacking and H-bond interaction between the acid chain-ends, when it exists. This double aggregation mechanism agrees with recent results published by our group [43,44] and they are strong enough to keep the stack architecture in place during the simulation time at 298 K. In Fig. 3, one can find the RDFs for a total of 8 molecules each (the cases containing 2 and 5 molecules each can be found in the ESI). In Fig. S2 one can find the final snapshots of these configurations.

A13 and C5Pe asphaltene molecules do aggregate under these thermodynamic conditions whereas porphyrin ones are spread all over the simulation box without any special aggregation pattern, as it can be seen from the RDFs and the snapshots. C5Pe, having acid chain-ends, can form structures based on the H-bond interactions and this is not the case of A13, which has CH_3 chain ends: this molecule can only aggregate forming π-stacks.

Then, the aggregation pattern of the asphaltene molecules in the presence of porphyrins was studied by adding to the simulation boxes containing 2, 5 or 8 asphaltene molecules only 1 porphyrin molecule. For the case of boxes containing 8 asphaltenes, other systems containing 2 or 3 porphyrins were also simulated. The concentration obtained in this way corresponds to the empirical evidences of metal concentration in the asphaltenic fraction of crude oil that are as high as ~500 ppm, what is equivalent to 1 porphyrin molecule to each 5–8 asphaltene molecules [13,37,38,58].

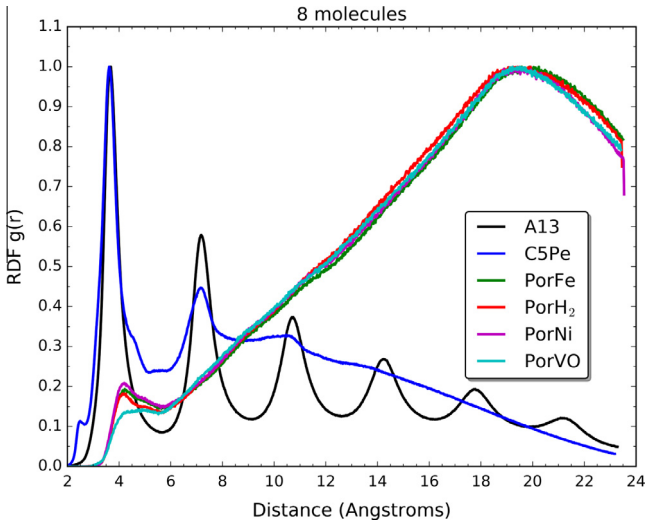

Fig. 3. RDFs for 8 molecules of A13, C5Pe, $PorH_2$, PorNi, PorFe, PorVO each interacting with themselves in $5 \times 5 \times 5$ nm^3 simulation boxes. One can clearly note that porphyrins have no aggregation pattern among them, the probability of face-to-face π-stacking aggregation (bump centered at 4 Å) being ten times smaller than the random distribution inside the box.

The RDFs of these systems are of two types and represent the asphaltene-asphaltene interaction and the asphaltene-porphyrin interaction. For the case where there is more than one porphyrin molecule, there is a third type of function representing the porphyrin-porphyrin interactions. In Fig. 4 one can find these curves for the 8 asphaltene molecules plus 1 porphyrin molecule case system. The other situations can be found in the ESI. These curves indicate that, while asphaltene molecules have a high probability of interacting among them forming organized structures in the case of A13 molecule (sharp peaks spaced equally indicating the π-stacking interactions) and less organized ones for the case of C5Pe (due to the presence of H-bonds between —COOH chain-ends which induces the widening of the peaks), the interaction with porphyrins is erratic and not constant across all the type herein studied. For A13 interacting with these metallic centers, PorFe is the only one presenting an important affinity with the asphaltene molecule, followed by PorNi. The other two porphyrins, the free-base, $PorH_2$, and the vanadyl one, PorVO, do not interact in any particular way with this molecule. We believe that this very ordered pattern observed for PorFe is because since the beginning this molecule was trapped in-between two asphaltene planes and kept this configuration throughout the whole simulation. Snap-

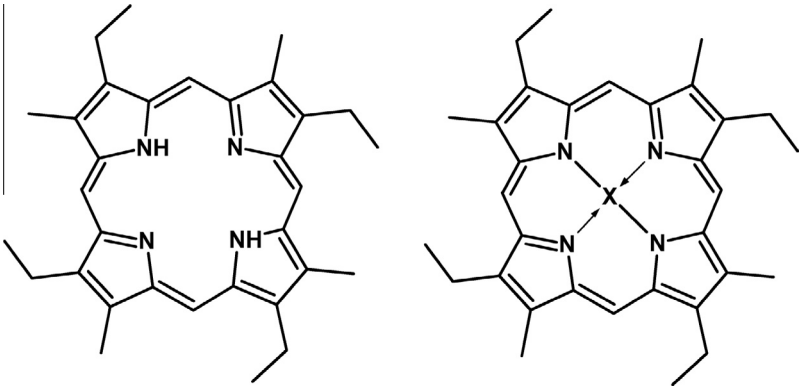

Fig. 2. Molecular structure of the porphyrins herein studied: (left) with no metal (free-base) ($PorH_2$) and metallic ones (right). **X** can be: **Ni**, **Fe** or (**VO**)$^{\bullet}$ (PorNi, PorFe and PorVO, respectively).

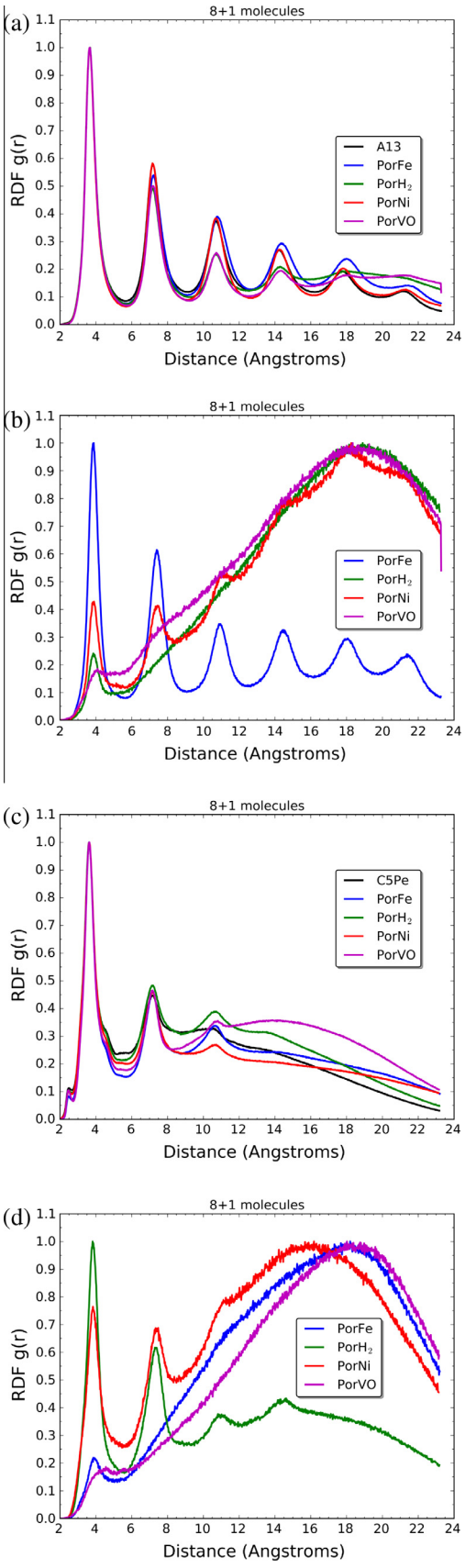

Fig. 4. RDFs for 8 molecules of A13 or C5Pe interacting with themselves or with each type of porphyrin herein studied: (a) A13 interacting with other A13 molecules when there is no porphyrin (black curve) or in the presence of one porphyrin of each type; (b) A13 molecule interacting with a porphyrin one of each type; (c) same as (a) but for C5Pe; and (d) same as (b) but in the case of C5Pe.

shots of the final configuration can be found in Figs. S2 and S3. For C5Pe asphaltene, the situation is quite the opposite: whereas PorVO continues not interacting with the asphaltene molecules, $PorH_2$ and PorNi are now the porphyrins with the greatest probabilities of interacting in a face-to-face configuration with a C5Pe molecule. On the basis of these curves, PorFe has now no pronounced affinity with the asphaltene molecule. The snapshots of the final simulation frame indicate that only C5Pe-$PorH_2$ system is stable in a co-facial architecture at this step of the simulation, as it can be seen in Fig. 5(a).

When the porphyrin concentration is increased, a clearer aggregation pattern can be identified, as it can be seen in Figs. S9 and S10. One can now clearly identify the probability of one porphyrin having a co-facial interaction with an asphaltene molecule (regardless of the type) up to the 5th neighbor. This indicates that the porphyrin is located on the top or in-between the stack. This probability density is higher for the systems containing A13 than the ones containing C5Pe and this should be due to the fact that C5Pe molecules do not always organize themselves as stacks, what is a consequence of the presence of acid chain-ends. This is better seen in the "8+3" systems' 60 ns snapshots presented in Fig. S4(a) and (b). In (a) one can see the presence of non-bonding interactions for the A13-PorNi "8+3" system, showing the close distance that the nickel atom can be from the aromatic hydrogen atoms of the conjugated backbone. This non co-facial interaction can explain the widening of the RDF peaks. Moreover, in (b), one can identify for the C5Pe-$PorH_2$ "8+3" system the insertion of the porphyrin molecule in-between planes of the asphaltene molecules.

Another interesting fact is that PorVO porphyrin does not interact significantly with any type of asphaltene molecule in a co-facial configuration. This may be due to two major factors: 1 - our attempt to translate the conformation properties of this molecule into classical parameters and their adaptation to the force field is not fruitful or; 2 - as this molecule is not planar (the VO center assumes a pyramidal conformation related to the plane of the tetrapyrolic macrocycle), it can not be inserted in-between the stacks as the other porphyrins can. The effect of both factors would induce a reduction of the probability of finding PorVO in the vicinity of an asphaltene molecule (see Fig. 5(b) and (c)). However, this does not avoid the interaction between the very polar oxygen atom of the VO group and other hydrogen atoms within the asphaltene molecules. Two distinct cases can be found in this situation: a - interaction with the —COOH group and b - interaction with the aromatic hydrogen atoms of the conjugated backbone. As it can be seen from Fig. S5(a), the first case has an average distance of interaction of 0.16 nm (peak not available in the RDFs - only the region higher than 0.2 nm is shown). The second case, identified by a bump in the RDF centered around 0.45 nm can be visualized in Fig. S5(b).

With all that said, CMDS do not show any strong interaction mechanism of aggregation between porphyrins and asphaltene molecules. This result is valid for the case where the porphyrin molecules do not present acid chain-ends. In this case, one would see that the aggregation is favored based on the H-bonds that can be formed between the porphyrins and the asphaltene molecules, as it is the case of asphaltenes having this type of chain-end [44]. In order to investigate whether these results arise from this fact or if there is indeed a deep electronic effect that has not been taken into account by CMDS, we performed DFT and PM7 calculations as well, as it can be found in the next section.

3.2. DFT and PM7 calculations

DFT and PM7 calculations are two distinct levels of theory that allow, in opposition to CMDS, the inclusion of the electrons in the calculation scheme. The treatment of the electronic cloud is neces-

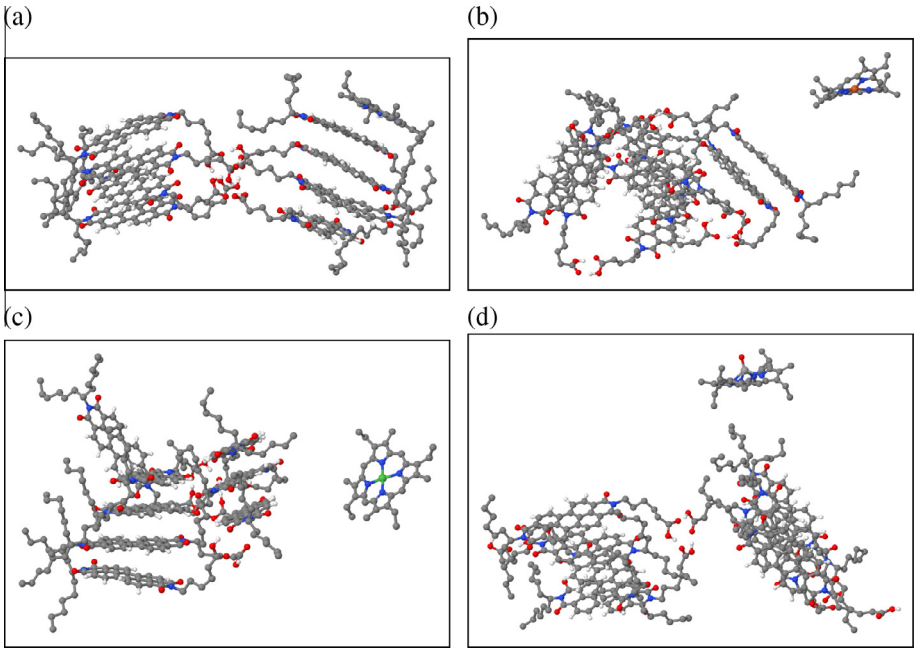

Fig. 5. 60 ns snapshots of the C5Pe interacting with (a) $PorH_2$, (b) PorNi, (c) PorFe, and (d) PorVO molecules in $5 \times 5 \times 5$ nm^3 simulation boxes. Toluene molecules are omitted for clarity.

sary to determine both if the force field used in the CMDS is accurate enough for the properties in interest and to better understand the origin of the physical-chemical mechanisms taking placing in the aggregation. Particularly in our case, the treatment of the vanadyl radical needs such methods. Finally, the differences between them is the fact that PM7 is a semi-empirical method that relies on the fitting of its internal parameters to make them reproduce properties obtained experimentally or from higher-levels of theory for a ensemble of test molecular systems. DFT, on the other hand, can have some degree of fitting but this is only used to tune the exchange-correlation functional.

In this way, all-electron DFT and PM7 calculations were performed in order to 1 - determine the electronic properties of the studied porphyrins in vacuum (DFT) and, 2 - to scan the "vertical" distance relevant to the aggregation mechanism (DFT), and 3 - optimize the internal coordinates for the minimum distance of interaction (PM7). Given the high computational cost of the methodology in use for these DFT calculations (B3LYP exchange-correlation functional with def2-TZVPP basis set and using the Stefan Grimme's D3BJ van der Waals correction - see ESI for more details), we have introduced the following approximations/constraints: 1 - for DFT calculations, we only considered the interaction between C5Pe and the 4 studied porphyrins since symmetry could be used; 2 - the lateral chains of the asphaltene molecules were reduced to a methyl group; 3 - the lateral chains of the porphyrins were set to a single hydrogen atom; and 4 - once the individual geometries of either C5Pe or the porphyrins optimized in vacuum, the interaction between them was studied by single-point calculations. The optimization of the minima were only performed within PM7 methodology. In this part of the modeling procedure, the iron porphyrins (PorFe) were not treated since their ground state is not the singlet one S_0 (it can be either triplet T_0 or quintuplet Qu_0). This has no incidence on the results obtained by CMDS since it does not take into account electrons explicitly. On the other hand, the presence of high-order spin states for the iron-compounds introduce more difficulties in our procedure since it would require treating multi-reference states, what is way beyond the capabilities of both DFT and PM7.

In this way, considering the isolated porphyrin molecules, the first astonishing pieces of information that can be extracted is the non-planar configuration of PorVO: the VO assumes a pyramidal structure above the macrocycle plane. Furthermore, the oxygen is pronouncedly negatively charged compared to the rest of the molecule. This can have as consequence both the non-possibility of introduction of this porphyrin between adjacent asphaltene planes and the possibility of forming new hydrogen interactions between acid chain-ends or aromatic hydrogens of the conjugated backbone, as already mentioned before. Besides having this pronounced charge, the PorVO molecule also has an unpaired electron which could have an effect on the aggregation of the asphaltene-porphyrin systems. This effect would not be taken into account by CMDS based on the classical character of this latter. This unpaired electron is delocalized over the VO bond region as it can be seen from Fig. S12, and the Mulliken spin population shows that the unpaired electron is distributed between the nitrogen ($\sim$−0.024), vanadium ($\sim$1.20) and oxygen ($\sim$−0.14) atoms.

These isolated porphyrins were centered around the origin lying planar on the *x*-*y* plane. The same alignment was also imposed to the C5Pe molecule, with its biggest axis lying parallel to *x* axis. The *z* axis was then scanned by single points from 6.0 down to 2.5 Å with 21 equally spaced distance steps. This was performed for the following systems: C5Pe-C5Pe, C5Pe-$PorH_2$, C5Pe-PorNi, and C5Pe-PorVO. The resultant attraction-repulsion potential curves in the neutral singlet state S_0 can be visualized in Fig. 6. These curves were fitted to a Morse potential and the obtained equilibrium energies are listed in Table 1.

Although the difficulties that are introduced by the ground state in higher spin states of the iron porphyrin, we have tried to estimate this energy of interaction for the triplet state (which is the ground state of the isolated porphyrin). More details can be found in the ESI. For the C5Pe-PorVO system, we first expected that the unpaired electron of the latter would induce the formation of a "covalent-like" bond with the asphaltene in a cation-π-like interaction, based on the fact that the radical can be considered as an electron poor species. The binding energy that was found is coherent with the ones for the other porphyrins and, besides, based on

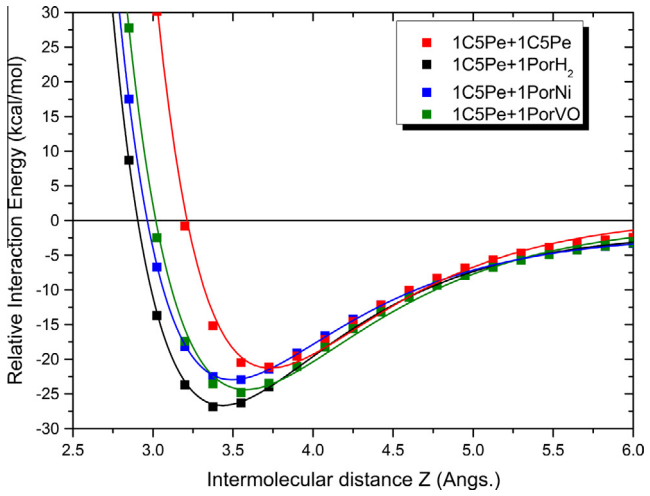

Fig. 6. Attraction-repulsion curves for the C5Pe-C5Pe, C5Pe-PorH_2, C5Pe-PorNi, and C5Pe-PorVO in S_0 state (D_0 for C5Pe-PorVO) calculated within the DFT level of theory.

Table 1
Energy of interaction ΔE for each C5Pe-porphyrin pair calculated by DFT and by PM7 $\Delta_f H^o_{298K}$, measured by the difference in the heat of formation.

Mol. 1	Mol. 2	ΔE (kcal mol^{-1})	$\Delta_f H^o_{298K}$ (kcal mol^{-1})
C5Pe	C5Pe	−21.3	−40.8
C5Pe	PorH_2	−26.7	−35.1
C5Pe	PorNi	−23.0	−20.1
C5Pe	PorVO	−24.6	−36.2

the plot of the localization of this unpaired electron as it can be seen in Fig. S13, it continues localized in the same region as it is found in the isolated molecule.

In this way, we could show that the interaction between porphyrins and asphaltene molecules are probable to happen but its intensity is not much greater than an asphaltene-asphaltene interaction. Even though CMDS and DFT results agree, i.e., the interaction exists but is not much stronger than what a single π-stacking would be, and that is why an optimization of the equilibrium distances of the DFT scanning curve was performed within the PM7 level of theory in order to obtain a still more stable energy. These results confirm both CMDS and DFT: the interaction between porphyrins and asphaltene molecules is not stronger than asphaltene-asphaltene interactions and this is due to the fact that the aromatic conjugated core is smaller than the ones of asphaltene molecules. The metalloporphyrins, such as PorNi and PorVO, interact differently with each type of asphaltene molecule and this should be a function of the symmetry of the conjugated core. These observations are consistent with practical observations which have shown that, when asphaltenes are dispersed in some solvents at room temperature, porphyrins can be released into the maltene's phase. These porphyrins can then be associated to these interacting weakly with the asphaltene nano-aggregates by $\pi - \pi$ interactions.

Besides the energy of interaction and the visualization of the localization of the unpaired electron on PorVO species, it would be interesting to visualize the non-covalent interaction beyond the quantification. To do so, we have used the Non-Covalent Interactions (NCI) formalism developed by Johnson and coworkers,[59] which is described in more details in the ESI, where one can also find, in Fig. S14, the plot of the electronic reduced gradient density s against the density ρ times the sign of λ_2. This analysis allows one to state that the differences between the C5Pe-C5Pe, C5Pe-PorH_2, C5Pe-PorNi and C5Pe-PorVO are noticed for the systems containing metals, which have besides this a peak centered associated to a bonding non-covalent Coulomb interaction (attractive) mediated by the presence of the metallic center.

More particularly, as it is showed in Fig. S16 and suggested by the CMDS calculations, we observed the existence of an attractive potential between the vanadyl group and hydrogen atoms calculated by DFT. This interaction energy between the VO···H pair strongly supports the hypothesis of an attractive interaction allowing a two-dimensional translational diffusion of the maltenes molecules at proximity of the slowly rotating asphaltene nanoaggregates with embedded PorVO radicals. We have shown several experimental evidences of such anisotropic molecular dynamics by our NMRD profiles [41], in particular a very long correlation time (~1 μs) of residence of such maltene at proximity of the asphaltene nanoaggregates. However, all the theoretical models that we develop for interpreting the striking observed bilogarithmic dispersion profiles in crude oils required an attractive potential energy for the maltene-asphaltene systems. Last but not least, the fact that PorVO assumes a tridimensional pyramidal geometry (see Figs. S12 and S13) due to the vanadyl group supports the choice of the NMR parameters in our previous works: distance of minimal approach between maltene proton and paramagnetic sources of relaxation VO^{2+} ions) needed for interpreting the NMRD data (see Fig. 7 for further explanation) [41]. This particular geometry of the PorVO molecule does not allow its insertion in-between planes of asphaltenes, in a "sandwich"-type conformation, as it can be the case for the other porphyrins, as it was herein showed. Instead, besides this attractive VO···H behavior, the insertion of these porphyrins should take place in the space between nanoaggregates of asphaltenes or in a way of displacing them from a perfect face-to-face $\pi - \pi$-stacking conformation.

4. Conclusions

We have shown using classical molecular dynamics simulations that the asphaltene-porphyrin aggregation phenomena is less dependent on the $\pi - \pi$-interaction type and should somehow depend more strongly on the H-bond formation between lateral chains of both compounds. This result was herein evidenced based on classical molecular dynamics, density functional theory and semi-empirical simulations showing that $\pi - \pi$ interactions are not strong enough to explain the fact that porphyrins are commonly found within asphaltene aggregates. In this way, besides interaction between lateral chains (which are out of the scope of this work), the nature of the $\pi - \pi$ asphaltene-porphyrin interaction was studied and found to be consistent with a van der Waals dispersion type with an important contribution of an attractive-repulsive Coulomb interaction between the metal and the asphaltene molecules. This former can be understood as a "cation-π" interaction type.

More particularly, for the vanadyl-centered porphyrins, their geometrical properties impose that they cannot be found in-between two asphaltene planes in a "sandwich"-like configuration. This corroborates the previous NMRD experiments that indicated a particular dynamics of maltene's protons in the proximity of the paramagnetic source of relaxation. This observation was herein explained based on both the geometrical model of the PorVO porphyrins and on the discovery of a strong attractive potential between this metallic center (namely, the oxygen atom of the VO^{2+} group) and environmental hydrogen atoms.

Finally, this also explains why porphyrins can be found in a wide range of molecular weights of asphaltene aggregates: 1 - some of them, such as the nickel-containing ones, can be found trapped in-between asphaltene planes in a "sandwich"-type con-

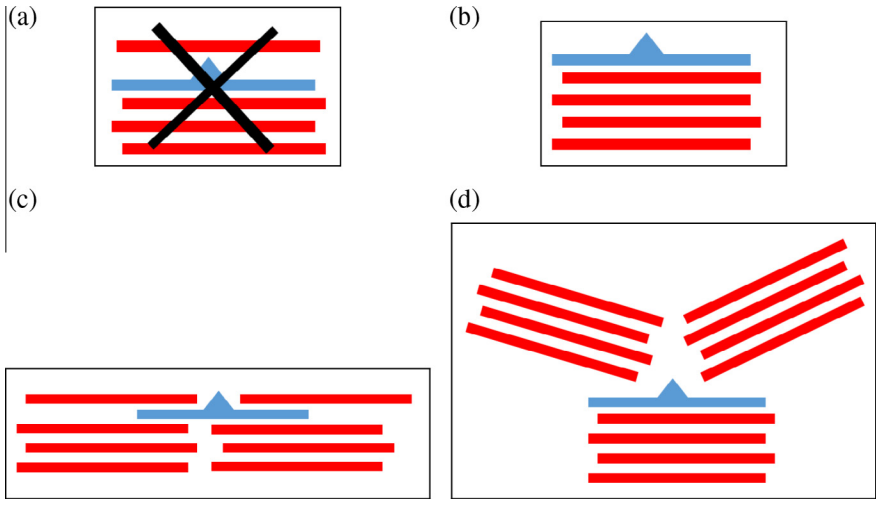

Fig. 7. Geometrical model of the interaction between PorVO and an asphaltene nanoaggregate. (a) PorVO is located in between two asphaltene planes. This is hypothesized not to take place because of the pyramidal geometry of the metallic center. (b) PorVO molecules can be found "sitting" on the asphaltene nanoaggregate (this interaction strength was calculated in this paper). (c) Due to its attractive potential towards hydrogen atoms, PorVO molecules can be found in between two nanoaggregates, unifying them. (d) Same as before but now the metallic centers interact with more than one nanoaggregate. One should note that maltenes can bidimensionally interact with the metallic center as previously showed by our NMRD data in situations (b) and (c).

figuration; 2 - others, such as the vanadium containing ones, can be found either sitting on the top of nanoaggregates or in-between different nanoaggregates interacting with their lateral chain's hydrogen atoms (the lateral chain only of an asphaltene can indeed be considered as a maltene); and 3 - these porphyrins can be found in close interaction with asphaltene nanoaggregates if acid lateral chains are grafted to them.

Acknowledgments

This work was performed using HPC resources from DN (Direction du Numérique) from Université de Pau et des Pays de l'Adour, the Mesocentre de Calcul Intensif Aquitain and from GENCI-CINES (Grant 2016-c2016087698). ISIFoR - Carnot Institute is acknowledged for its financial support.

Appendix A. Supplementary material

Supplementary data associated with this article can be found, in the online version, at http://dx.doi.org/10.1016/j.fuel.2016.10.065.

References

[1] Liu SK. Refining heavy crude oil by distillation, deasphalting bottoms stream, oxidizing asphaltic residue to produce synthesis gas, reacting carbon monoxide with steam to produce hydrogen, using in hydrotreating process. US Patent 5958365; 1999.
[2] Speight JG. Petroleum chemistry and refining. CRC Press; 1997.
[3] Que G, Men C, Meng C, Ma A, Zhou J, Deng W, et al. Heavy oil hydrocracking process with multimetallic liquid catalyst in slurry bed. US Patent 6660157; 2003.
[4] Olsen D, Ramzel EB. Fuel 1992;71:1391–401.
[5] Dunning H, Moore J, Denekas M. Indust Eng Chem 1953;45:1759–65.
[6] Groennings S. Anal Chem 1953;25:938–41.
[7] Dunning H, Moore J, Myers A. Indust Eng Chem 1954;46:2000–7.
[8] Dunning H, Rabon NA. Indust Eng Chem 1956;48:951–5.
[9] Boduszynski MM. Energy Fuels 1988;2:597–613.
[10] Mullins OC, Kaplan M. J Chem Phys 1983;79:4475–88.
[11] Dickson F, Kunesh C, McGinnis E, Petrakis L. Anal Chem 1972;44:978–81.
[12] Qian K, Mennito AS, Edwards KE, Ferrughelli DT. Rapid Commun Mass Spectrom 2008;22:2153–60.
[13] McKenna AM, Purcell JM, Rodgers RP, Marshall AG. Energy Fuels 2009;23:2122–8.
[14] Adams JJ. Energy Fuels 2014;28:2831–56.
[15] Mullins OC, Sheu EY, Hammami A, Marshall AG. A sphaltenes, heavy oils, and petroleomics. Springer Science & Business Media; 2007.
[16] Benamsili L, Korb J-P, Hamon G, Louis-Joseph A, Bouyssiere B, Zhou H, et al. Energy Fuels 2013;28:1629–40.
[17] Mullins O, Groenzin H. J Phys Chem A 1999;103:11237–45.
[18] Boduszynski MM. Am Chem Soc, Div Pet Chem, Prepr. United States; 1979 [24 year].
[19] Mullins OC. Energy Fuels 2010;24:2179–207.
[20] Mullins OC. Ann Rev Anal Chem 2011;4:393–418.
[21] Sabbah H, Morrow AL, Pomerantz AE, Zare RN. Energy Fuels 2011;25:1597–604.
[22] Barré L, Jestin J, Morisset A, Palermo T, Simon S. Oil Gas Sci Technol-Revue de l'IFP 2009;64:617–28.
[23] Groenzin H, Mullins OC. J Phys Chem A 1999;103:11237–45.
[24] Groenzin H, Mullins OC. Energy Fuels 2000;14:677–84.
[25] Hodgson G, Hitchon B, Taguchi K, Baker B, Peake E. Geochim Cosmochim Acta 1968;32:737–72.
[26] Kim S, Rodgers RP, Blakney GT, Hendrickson CL, Marshall AG. J Am Soc Mass Spectrom 2009;20:263–8.
[27] Stanford LA, Rodgers RP, Marshall AG, Czarnecki J, Wu XA. Energy Fuels 2007;21:963–72.
[28] Shi Q, Hou D, Chung KH, Xu C, Zhao S, Zhang Y. Energy Fuels 2010;24:2545–53.
[29] Liu H, Mu J, Wang Z, Guo A, Chen K. Energy Fuels 2016;30:1997–2004.
[30] Caumette G, Lienemann C-P, Merdrignac I, Bouyssiere B, Lobinski R. J Anal Atomic Spectrom 2009;24:263–76.
[31] Dunning H, Moore J, Bieber H, Williams R. J Chem Eng Data 1960;5:546–9.
[32] Howe WW. Anal Chem 1961;33:255–60.
[33] Morandi J, Jensen H. J Chem Eng Data 1966;11:81–8.
[34] Grigsby R, Green J. Energy Fuels 1997;11:602–9.
[35] Qian K, Edwards KE, Mennito AS, Walters CC, Kushnerick JD. Anal Chem 2009;82:413–9.
[36] Mullins OC, Seifert DJ, Zuo JY, Zeybek M. Energy Fuels 2012;27:1752–61.
[37] Caumette G, Lienemann C-P, Merdrignac I, Bouyssiere B, Lobinski R. J Anal Atomic Spectrom 2010;25:1123–9.
[38] Barbier J, Marques J, Caumette G, Merdrignac I, Bouyssiere B, Lobinski R, et al. Fuel Process Technol 2014;119:185–9.
[39] Delpoux O, Barbier J, Marques J, Verstraete J, Vezin H. In: Proceedings of the 14th international conference on petroleum phase behavior and fouling, petrophase, Poster PB33, Rueil-Malmaison, France.
[40] Korb J-P, Louis-Joseph A, Benamsili L. J Phys Chem B 2013;117:7002–14.
[41] Korb J-P, Vorapalawut N, Nicot B, Bryant RG. J Phys Chem C 2015;119:24439–46.
[42] Eyssautier J, Levitz P, Espinat D, Jestin J, Gummel J, Grillo I, et al. J Phys Chem B 2011;115:6827–37.
[43] Sodero ACR, Santos-Silva H, Guevara Level P, Bouyssiere B, Korb J-P, Carrier H, et al. Energy Fuels 2016;30(6):4758–66.
[44] Santos-Silva H, Sodero ACR, Bouyssiere B, Carrier H, Korb J-P, Alfarra A, et al. Energy Fuels 2016;30(7):5656–64.
[45] Schulze M, Lechner MP, Stryker JM, Tykwinski RR. Organ Biomol Chem 2015;13:6984–91.
[46] Scheidt WR, Reed CA. Chem Rev 1981;81:543–55.
[47] Pasternack RF, Gibbs EJ. Metal ions in biological systems: volume 33: probing of nucleic acids by metal ion complexes of small molecules, vol. 33; 1996. p. 367.
[48] Marques HM, Munro OQ, Grimmer NE, Levendis DC, Marsicano F, Pattrick G, et al. J Chem Soc, Faraday Trans 1995;91:1741–9.

[49] Sundar VC, Sontum SF. Middlebury (VT): Middlebury; 1997.
[50] Strausz OP, Mojelsky TW, Lown EM. Fuel 1992;71:1355–63.
[51] Gao F, Xu Z, Liu G, Yuan S. Energy Fuels 2014;28:7368–76.
[52] Teklebrhan RB, Ge L, Bhattacharjee S, Xu Z, Sjöblom J. J Phys Chem B 2014;118:1040–51.
[53] Schuler B, Meyer G, Peña D, Mullins OC, Gross L. J Am Chem Soc 2015;137:9870–6.
[54] Stewart JJ. J Mol Model 2013;19:1–32.
[55] Hostaš J, Řezáč J, Hobza P. Chem Phys Lett 2013;568:161–6.
[56] Dutra JDL, Filho MA, Rocha GB, Freire RO, Simas AM, Stewart JJ. J Chem Theory Comput 2013;9:3333–41.
[57] Thiel W. Wiley Interdisc. Rev.: Comput. Mol. Sci. 2014;4:145–57.
[58] Mullins OC, Martínez-Haya B, Marshall AG. Energy Fuels 2008;22:1765–73.
[59] Johnson ER, Keinan S, Mori-Sanchez P, Contreras-Garcia J, Cohen AJ, Yang W. J Am Chem Soc 2010;132:6498–506.